Modelling of Bracing in a Multi-Body Active Human Model

Riske Meijer[1], Jeroen Broos[1], Hala Elrofai[1], Edo de Bruijn[2], Patrick Forbes[2], Riender Happee[2]

Abstract The severity of occupant injuries sustained during automotive collisions can increase when an occupant is out-of-position prior to the crash. Several studies have shown that muscle activation significantly affects human kinematics in low severity impacts or pre-crash car movements. As such, it is important to quantify the influence of this behaviour to effectively design safety systems. Reactive behaviour can be simulated with a recently developed computer human model that stabilises to a predefined position. The objective of this study was to adapt this model to simulate realistic bracing behaviour during braking. A new neck model was developed as well as a new arm model. In an anterior-posterior frequency perturbation test the new neck model showed a more comparable response to that of a volunteer than the previous model. In arm pulse perturbation tests the new arm model showed comparable behaviour to a volunteer in relaxed as well as in braced conditions. Finally, a simulation of a braking event with the new active human model showed that bracing has a substantial effect on the head and thorax displacement. It is concluded that the new neck and new arm model improved the active human model for the development of active safety systems.

Keywords Active behaviour, arm, bracing, human modelling, muscles, neck

I. INTRODUCTION

The severity of occupant injuries sustained during automotive collisions can increase when an occupant is out-of-position prior to the crash [1]. Scenarios such as rollover, extreme vehicle motion or secondary human tasks move the occupant away from the posture for which the restraint systems were optimally designed. Recent developments in occupant safety focus on active systems, that respond moments before the crash to correct the occupant's position or deploy safety measures that account for occupant position. For example, a reversible belt pretensioner has been designed to pull the occupant rearward to optimise the occupant position prior to frontal crashes and a seat that acts with a pre-pulse to reduce the load on the occupant during the crash [2][3]. Similarly, a reactive reversible belt pre-pretensioner has been designed to reduce occupant movement in highly dynamic driving situations to increase safety in frontal, rearward and lateral crashes [4].

However, bracing and/or reactive behaviour prior to impact can introduce confounding factors; the resultant muscle activation can significantly affect the kinematics in low severity impacts or pre-crash conditions. Volunteer sled tests indicate that when subjects brace, forward head excursion decreases by approximately 47% and 36% during frontal impacts at 2.5 and 5 G respectively [5]. When occupants are instructed to resist an oncoming braking acceleration, lumbar flexion decreases and neck flexion is effectively eliminated [6]. Head excursion and neck flexion during voluntary braking are substantially reduced relative to equivalent surprise autonomous braking [7] indicating the relevance of anticipatory postural reactions.

Active systems can make use of the fact that occupants are able to brace to reduce motion, for example, by means of giving a warning signal prior to an oncoming crash. However, occupant reaction characteristics and reaction times to a warning signal may differ. In order to evaluate the real-world effect of active safety systems during the pre-crash phase as well as during the crash phase, the various responses of occupants should be taken into account. For this a run-time efficient multi-directional computer human model that can stabilise to the initial or a predefined position has been developed [8]. The active components within the model include bracing (i.e. co-contraction) with variable reaction times and reflexive stabilisation. This active human model showed to be capable of simulating the kinematics of volunteers [8][9] during a 1 g car braking event [10], 3.8 g

[1]) Riske Meijer (riske.meijer@tno.nl, Tel. +31 888665753), Jeroen Broos and Hala Elrofai are Research Scientists at TNO, Netherlands Organisation for Applied Scientific Research.
[2]) Edo de Bruijn and Patrick Forbes are PhD students, and Riender Happee is Assistant Professor at Delft University of Technology.

sled frontal impact with 3-point belt [11], 15 g frontal impact with a 5-point belt [12], 7 g lateral impact with a 5-point belt [13], and 3.6 g rear impact without belt [14]. It also showed to be capable of simulating the responses of post mortem human subjects in published blunt impact tests [9] on the head [15], thorax [16]-[21] and abdomen [22] at several loading conditions. In the volunteer tests the bracing induced co-contraction levels needed for the head peak displacements to match the response corridors were 0.5-0.9 (on a scale from 0-1). These co-contraction levels seem rather high when considering that the volunteers in these tests were not instructed to brace. Furthermore, for driver simulations this model lacks the possibility to simulate bracing of the arms, which is expected to have a significant effect on the forward excursion of the thorax [23][24].

The objective of this study is to adapt the active human model to simulate realistic bracing behaviour during braking. For this the neck model is improved by implementing a new dataset set of muscles from a 50th percentile post mortem human subject. The dynamic behaviour of the new neck model is evaluated through comparison against volunteer responses during anterior-posterior perturbation experiments. Arm bracing is incorporated and evaluated by means of volunteer arm pulse perturbation tests. Finally, the effect of bracing in a braking event is simulated by comparing the response of the new active human model in a relaxed and in a braced condition.

II. METHODS

The Active Human Model

Details of the original development of the active human model are provided in [8]. The model in a braking situation is shown in Fig. 1. The active human model that was used as a starting point in this study is version 1.1 [25] in the multi-body and finite element software package MADYMO version 7.4.1 [26]. A brief description of this model is provided below.

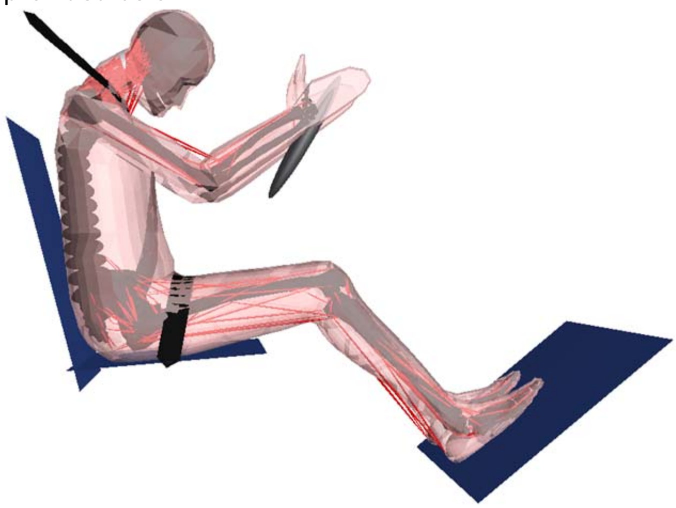

Fig. 1. Active human model in a braking situation.

For run-time efficiency, and for focusing on kinematic responses and global injury criteria, multi-body modelling techniques are used in this model. Hill-type muscle elements [27] are included in the neck, arms and legs to model active behaviour. The muscle elements have a realistic curvature that is maintained during movements. Due to the complexity of the spinal musculature, active behaviour of the lumbar and thoracic spine is modelled using actuators on the vertebral joints.

Sensors throughout the model measure the current rotation of the head, elbows, hips and vertebrae (representing muscle spindle feedback). Also, a target signal is defined which can be changed, but which by default is 0 in order to stabilise towards the initial position. The control error is calculated as the difference between the sensor and target signals. A reaction time is implemented that represents the time it takes for the human brain to start responding to any new event. This includes the time needed for sensing, transfer of the signal to the brain, and processing in the brain. The reaction time is implemented such that:

- Control errors related to pure stabilising behaviour, without any new events, cause a response with a limited delay representing reflexive stabilisation;
- New events cause a response after an additional reaction time.

New events are automatically detected by the active human model. A new event is defined as any external load causing a control error that is larger than the maximum error occurred in the simulation up to the current time step. If the error remains below the maximum, the signal is transferred directly, but if the error is above the maximum, it is limited to the maximum during the reaction time before it increases further.

Proportional-integral-derivative (PID) controllers aim to reduce the error by calculating a correcting load and are in series with a neural time delay. The neural delay is defined as the time it takes for the signal transfer from the Central Nervous System (CNS) to the muscle and the time it takes for the muscle to convert the signal into a force. The neural delay is 40 ms for the neck muscle controllers, 70 ms for the spine actuator and arm muscle controllers, and 100 ms for the leg muscle controllers. The last step in the control system is different per body part, and explained below.

The neck controller acts in three degrees of freedom, being the three rotations of the head. Depending on the initial settings in the model, the head rotations are either calculated relative to the reference space, to keep the head upright in space, or relative to T1, to keep the neck straight. The muscle recruitment table translating the correcting load to individual neck muscle activation was taken from the model of [28]. This recruitment is balanced, which means that an error in one degree of freedom results in a torque in only that degree of freedom. Besides the control on the three degrees of freedom of the head, also co-contraction of the neck muscles can be defined. Co-contraction is the simultaneous tension of all muscles without giving any resultant torques.

The controllers of the elbows act in only one degree of freedom, being the elbow flexion-extension. The muscle recruitment for the elbow divides the muscles in a group of flexors and a group of extensors and activates all muscles in one group to the same extent.

The controllers of the hips act in three degrees of freedom, being the three rotations of the hip joint, flexion-extension, medial-lateral rotation and abduction-adduction. The muscle recruitment table for the hip is set up such that for any of the three predefined degrees of freedom the muscles that have most effect in that degree of freedom are activated the most.

For the spine no predefined positions are used. Hence, the rotation error for the spine is equal to the sensor output. The spine controller acts in three degrees of freedom per vertebra for each of the 5 lumbar and 12 thoracic vertebrae, so 17 vertebrae in total. For each vertebra sensors are defined to measure the angle of the vertebra relative to the sacrum (pelvis). The activation signal for each vertebra is then applied to that vertebra as well as to the vertebrae below, such that the spine is in a stable position.

New Neck Model

Since the co-contraction levels needed for the head peak displacements to match the response corridors were thought to be quite high [8] and some muscles were lacking in the neck model, the neck model was improved with a muscle data set from a recent study [29]. The study of [29] resulted in a complete muscle geometry and parameter dataset obtained from one 50th percentile male post mortem human subject for a total of 68 muscle parts divided into 258 elements. From that dataset the muscle attachment locations as well as physiological cross sections were used. The size of the vertebrae of the previous head-neck model was not altered and the neck was oriented in a neutral position. The new dataset was scaled to provide a best least-squares fit between 9 landmarks on both skulls. A scaling factor of 0.949 was applied to the muscles of the new dataset. A Veldpaus least-squares optimisation algorithm [30] was used to define a rotation matrix and translation vector for each vertebral body which minimised distances between respective bony landmarks. The landmarks used were the spinous process, left and right tuberculum anterior and posterior, and the left and right transverse processes. For C7 and C2 the tuberculums were missing, while C3-C6 did not have measured transverse processes. The model was sliced transversally at the different vertebrae and the locations of the muscles were matched with MRI data found on the online available dataset of the Visible Human Project [31]. Each muscle's total length was calculated in the neutral position and was defined as the optimal muscle length. The stiffness of the ligaments and intervertebral discs was adapted, as well as the passive bending stiffness of all vertebral joints. Finally, the muscle recruitment table was recalculated.

Evaluation of the New Neck Model

The dynamic behaviour of the model was evaluated through comparison to head-neck stabilisation responses of a volunteer during pseudorandom anterior-posterior torso perturbation experiments. Details of the experiments are available in [32] and a brief description is provided here. The volunteer was seated and restrained on a rigid chair fixed on a motion platform. The volunteer was instructed to take on a comfortable upright seating position, stabilise his head comfortably above the torso, and maintain visual focus on a stationary target 3 m in front of the platform. A quasi-random multisine [33] anterior-posterior perturbation signal was applied in translational direction. The signal was 20 s in length providing a frequency resolution of 0.05 Hz. It was designed to have flat power in velocity and a root-mean-square (RMS) velocity of 0.08 m/s. The lowest frequency was fixed at 0.3 Hz and the highest frequency was 1.2, 4, 6 or 8 Hz.

The stabilisation response of the volunteer throughout the perturbation was described by means of frequency response functions (FRFs). An FRF describes the dynamic behaviour (gain and phase) of a system as a function of frequency. The gain indicates the magnitude of the output relative to the input while the phase indicates the timing of the output relative to the input. The FRF used in this study was estimated for input torso velocity and output head velocity as (Equation 1):

$$\widehat{H}_{dy} = \frac{\hat{s}_{dy}(f)}{\hat{s}_{dd}(f)} \tag{1}$$

where d is the input velocity disturbance measured at the torso and y is the output head kinematics. The estimation of the FRFs assumes a linear relationship between the input and output signals.

Based on the head and neck geometry of the volunteers, a single volunteer was selected for the evaluation of the new neck model. The 8 Hz condition was used since it allows for an evaluation of the model dynamics across the widest bandwidth. This frequency perturbation volunteer test was simulated with the previous active human model and with the new active human model for comparison. In this simulation the joints below T1 were locked. The T1 displacement was prescribed as an input signal. No co-contraction of the neck muscles was applied. The FRF as well as the Fast Fourier Transform (FFT) of the simulation were calculated and compared to the test results.

New Arm Model

The previous active human model [8] is not able to actively brace the arm and to control the shoulder joint motion. Furthermore, the elbow joint is only able to control the flexion-extension motion and the biofidelity of the muscle activation recruitment table is limited. In the new active human model the motion of the shoulder and elbow joints are controlled in such a way that they try to maintain their initial position and are capable of bracing.

The arm muscles of the new model are described in Table I. The muscles that are connected to the hand are not controlled, so these muscles only affect the passive response of the arm model. In the new arm model two degrees of freedom of the elbow being flexion-extension and pronation-supination are controlled by the 7 contributing muscles. Similar as for the neck model a recruitment table was calculated which ensures that the elbow joint torques in flexion-extension and pronation-supination are balanced. The activation levels of the muscles which are needed to create the required force were determined using a minimal muscle fatigue strategy [34]. Stabilisation of the elbow joint can be simulated by using the activation parameter (0-1), and in addition a certain co-contraction level (0-1) is used to simulate bracing of the muscles. The co-contraction is balanced for any flexion-extension angle of the elbow and only added to the triceps and brachialis muscles to ensure stability in supination-pronation movement of the elbow. As a consequence, the elbow joint can only brace in flexion-extension movement.

To control the rotational movement of the humerus and translational movement of the scapula and clavicle, a shoulder joint control system was implemented which tries to maintain the initial position and orientation of the humerus with respect to the torso. Five actuators, controllers and sensors were implemented in each arm for the three rotational degrees of freedom of the glenohumeral joint and for the posterior-anterior and superior-inferior translational movement of the scapula and clavicle with respect to the thorax. Three actuators and sensors were implemented between the sternum and humerus to control the rotational movement of the humerus. Two actuators and sensors were implemented between the sternum and the scapula (placed at the glenohumeral joint location) to control the translational movement of the scapula and clavicle. Additional to these five stabilising controllers bracing of the shoulder joint is modelled by three rotational and two translational restraints between the sternum and the humerus and across the glenohumeral joint. These restraints give extra rotational as well as translational stiffness to the shoulder, as co-contraction does in the elbow muscles. The stiffness of these restraints is dependent on the co-contraction level defined for the whole arm of the active human model.

TABLE I
Muscle implementation in the active human model arm

Muscle	From	To	Joint	Elbow Motion
Triceps long head	Scapula	Ulna	Elbow	Extension
Triceps medial head	Humerus	Ulna	Elbow	Extension
Triceps lateral head	Humerus	Ulna	Elbow	Extension
Supinator ulna-radius	Ulna	Radius	Elbow + Radius-ulna	Flexion-supination
Supinator humerus-radius	Humerus	Radius	Elbow + Radius-ulna	Flexion-supination
Brachialis	Humerus	Ulna	Elbow	Flexion
Pronator teres	Humerus	Radius	Elbow + Radius-ulna	Flexion-pronation
Biceps brachii long head	Scapula	Ulna	Elbow + Radius-ulna	Flexion-supination
Biceps brachii short head	Scapula	Radius	Elbow + Radius-ulna	Flexion-supination
Extensor carpi radialis brevis	Humerus	Hand	Elbow + Radius-ulna	Flexion-supination
Extensor carpi radialis longus	Humerus	Hand	Elbow + Radius-ulna	Flexion-supination
Brachioradialis	Humerus	Radius	Elbow + Radius-ulna	Extension-supination
Flexor carpi radialis	Humerus	Hand	Elbow + Radius-ulna	Flexion-pronation
Pronator quadratus	Ulna	Radius	Radius-ulna	Pronation

Evaluation of the New Arm Model

The arm of the active human model was evaluated by simulating force pulse perturbation tests with a volunteer. Details of the experiments are available in [35] and a brief description is provided here. During these tests continuous and pulse perturbations were applied to the right hand of the volunteer by a robotic manipulator which was free to move in the horizontal plane. This manipulator acted as a linear mechanical system with mass-spring-damper properties. The volunteer was strapped by a four-point belt to a seat and the wrist was cuffed. The volunteer was asked to hold the handle of the manipulator while continuous and pulse perturbations were applied. Furthermore, the volunteer was asked to perform a position or a relaxed task. The instruction for the position task was to keep the handle on the initial position, and for the relaxed task to relax the arm. The pulses differed in direction (left or right). The relaxed task tests were performed with low severity pulse, while the position task tests were performed with low as well as with high severity pulse. Fig. 2 shows an example of the high and low severity pulses that were injected into the manipulator control loop. Due to the manipulator dynamics the actual forces at the hand load cell were much lower.

Two relaxed task and four position task pulse perturbation tests were simulated of a volunteer with similar arm size and mass as the active human model. In the simulations the mass, stiffness and damping properties of the manipulator were set to 3.27 kg, 21.0 N/m and 0.27 Ns/m, respectively [35]. The hand-handle connection was modelled by a spring-damper system with a stiffness of 22.4 N/m and a damping of 57.0 Ns/m [35]. To simulate the relaxed task test the activation level of the arm was reduced to 0.08, and no co-contraction was applied. Note that the reduced arm activation level of 0.08 is not a standard setting for the active human model, as the muscle control systems of the human model were developed to stabilise joints. The volunteer was not instructed to maintain the initial position in the relaxed task tests. Therefore, the arm activation level was reduced in the simulations of the relaxed task tests. To simulate the position task the muscle activation level was set to default (1), and additional arm muscle bracing was simulated by setting the co-contraction level to 0.3. The reaction time was set to 30 ms in all these simulations [35].

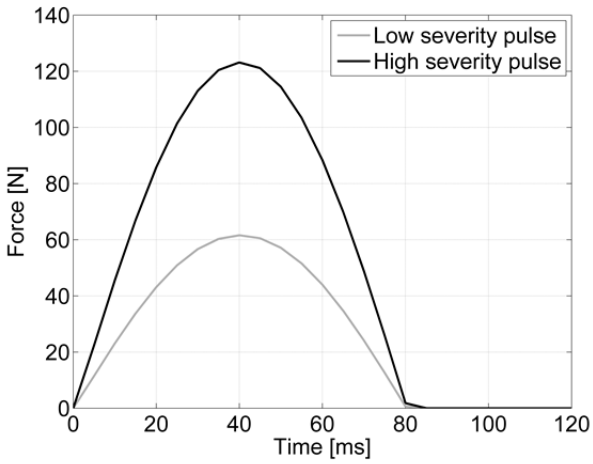

Fig. 2. Example of the low and high severity pulse of the arm pulse perturbation tests.

Evaluation of Bracing of the Active Human Model During Braking

In order to evaluate the effect of bracing of the new active human model, a braking event of a relaxed and a tensed case was simulated. For this the new active human model was settled in a rigid seat with a 3-point belt (without retractor), steering wheel and footplate. The applied braking pulse was 0.8 g during 600 ms. To simulate the relaxed case the activation parameter for all body parts was set to 1, except for the arms where it was set to 0.08, and the co-contraction level of the neck and arm muscles was set to 0. In the braced case the activation parameter for all body parts was set to 1, and the co-contraction level of the neck and arm muscles was set to 0.3. The reaction time was set to 30 ms in both cases. So, the settings for the arm models in the relaxed case are equal to that in the relaxed task as described in above section, and in the braced case equal to that in the position task. The resulting kinematics of the active human model in both cases were compared to each other.

III. RESULTS

Evaluation of the New Neck Model

Fig. 3 shows the amplitude of FFT of T1 calculated from the T1 velocity from the volunteer posterior-anterior frequency perturbation test, which was used as input for the simulation. In Fig. 4 the gain and the phase of the FRF of the head relative velocity of both the new and the previous active human model in the frequency perturbation test are compared to the volunteer results. At the lowest frequency the volunteer data and the two models show an FRF gain close to zero indicating a very limited head motion relative to T1, which can be attributed to effective neck stabilisation. At the highest frequency an FRF gain of one and a phase of -180° indicates that the head is stationary in space, mainly due to its inertial properties. The intermediate frequencies show a more complex behaviour attributed to reflexive and co-contraction based stabilisation. In Fig. 5 the amplitudes of the FFT of the head relative velocity for the same test are shown. The gain of the FRF and the amplitude of the FFT indicate that the neck muscles of the previous model show a stiffer response than the volunteer for low frequencies (< 2 Hz). On the other hand, the previous model shows a more compliant behaviour for higher frequencies than the volunteer, especially between 3 and 5 Hz. Thus, the new model shows an improved response compared to the previous model for all tested frequencies. Also, Fig. 4 shows that the phase (timing) better replicates the behaviour of the volunteer, especially for frequencies higher than 2 Hz.

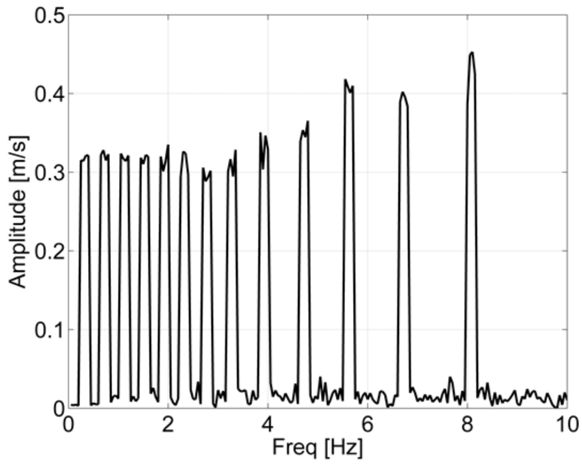

Fig. 3. Amplitude of FFT of T1 from the volunteer test, which is used as input for the simulation.

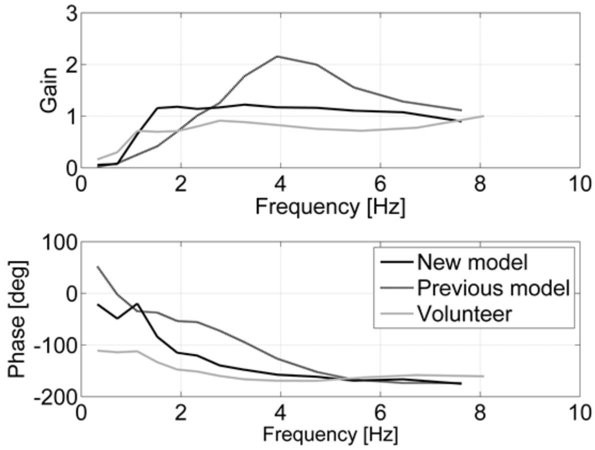

Fig. 4. Gain and phase of the FRF of head relative to T1 velocity of the volunteer, the new active human model and the previous active human model.

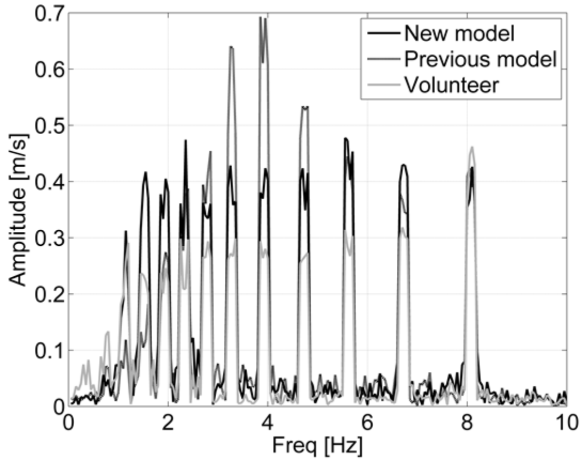

Fig. 5. Amplitude of FFT of head relative to T1 velocity of the volunteer, the new active human model and the previous active human model.

Evaluation of the New Arm Model

In Fig. 6 and Fig. 7 the displacement of the perturbator handle resulting from the simulations with the new active human model are compared to that of the volunteer in the relaxed task tests. These figures show that the new arm model in relaxed condition moves comparable that of the volunteer. For both the volunteer and the new active human model, the handle moved more in the tests with the pulse to the left than to the right.

In Fig. 8 to Fig. 11 the displacement of the perturbator handle of the simulations with the new active human model are compared to that of the volunteer tests in the position task tests. These figures show that the new arm model in braced condition moves comparable to that of the volunteer for both pulse severities. However, the movement to the initial position after the pulse to the right of the volunteer's arm is faster than that of the new arm model. Comparing the simulation and test results of the relaxed task (see Fig. 6 and Fig. 7) to that of the position task with the similar severity pulse (see Fig. 8 and Fig. 9), it is shown that bracing decreases the handle displacement in X-direction more than two times for the volunteer as well as for the new active human model. This indicates that the new active human model is capable of simulating arm bracing.

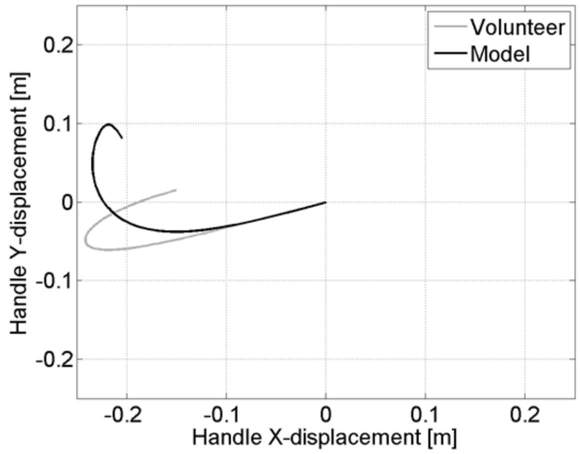

Fig. 6. Handle displacement of the volunteer and the new active human model during first 1000 ms of relaxed test with low severity pulse in left direction.

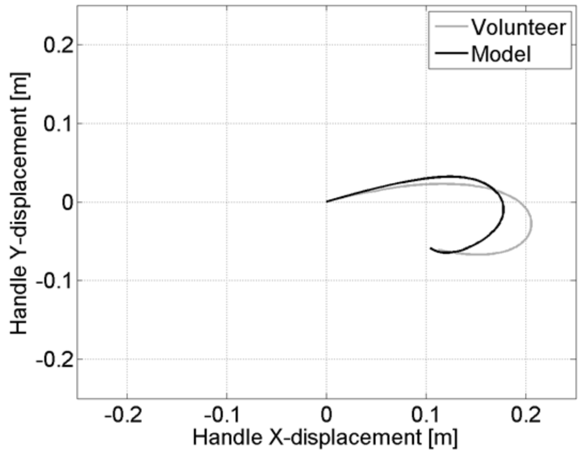

Fig. 7. Handle displacement of the volunteer and the new active human model during first 1000 ms of relaxed test with low severity pulse in right direction.

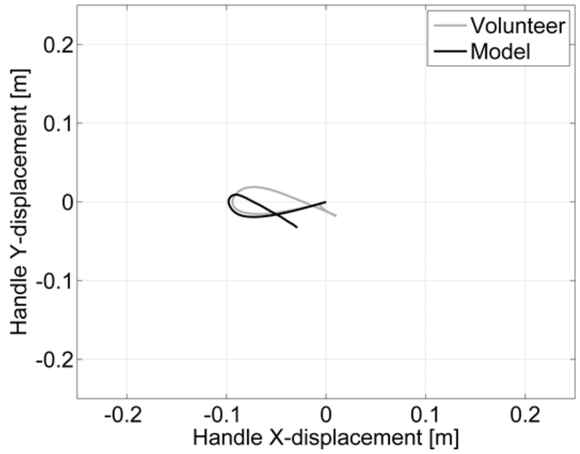

Fig. 8. Handle displacement of the volunteer and the new active human model during first 1000 ms of position task test with low severity pulse in left direction.

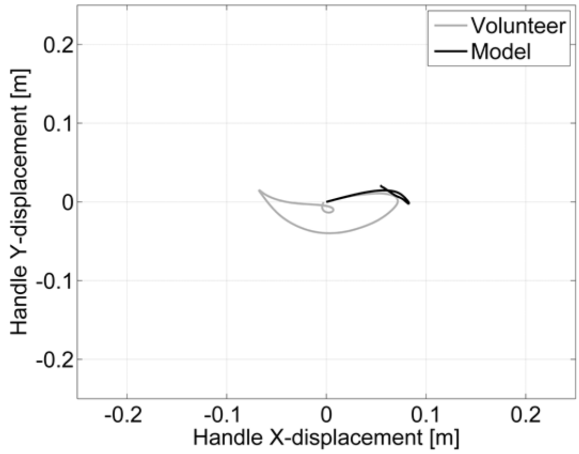

Fig. 9. Handle displacement of the volunteer and the new active human model during first 1000 ms of position task test with low severity pulse in right direction.

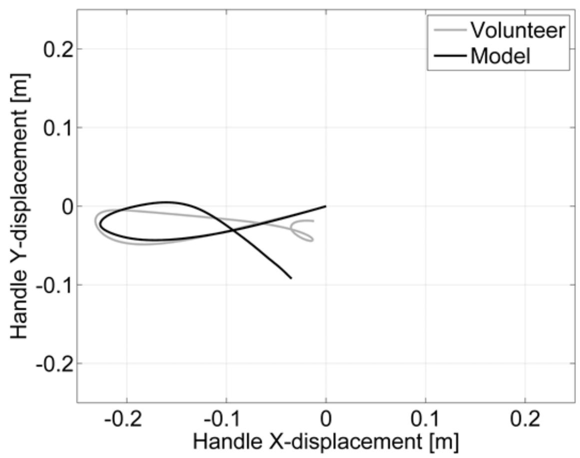

Fig. 10. Handle displacement of the volunteer and the new active human model during first 1000 ms of position task test with high severity pulse in left direction.

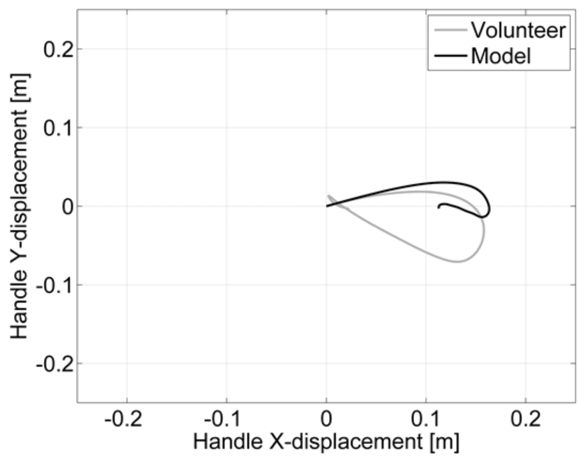

Fig. 11. Handle displacement of the volunteer and the new active human model during first 1000 ms of position task test with high severity pulse in right direction.

Evaluation of Bracing of the Active Human Model During Braking

Fig. 12 to Fig. 14 show the head and T1 displacement of the new active human model in the braking simulation of the relaxed and the braced case. Fig. 15 shows the new active human model in most forward displacement during the braking simulation of both cases. Fig. 12 shows that the head displacement is more than twice as much in the relaxed case than in the braced case. Fig. 13 and Fig. 14 show that the larger displacement of the head in the relaxed case is mainly caused by the larger T1 displacement. The T1 displacement is most affected by the bracing of the arms, since the activation of the spine and leg muscles was the same in both cases.

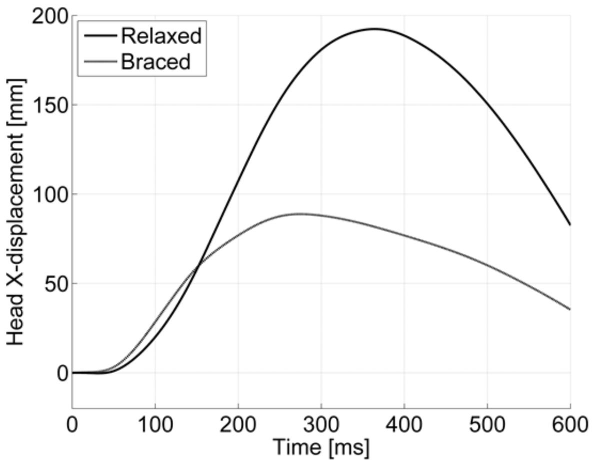

Fig. 12. Head forward displacement of the new active human model in simulation of a relaxed and braced case.

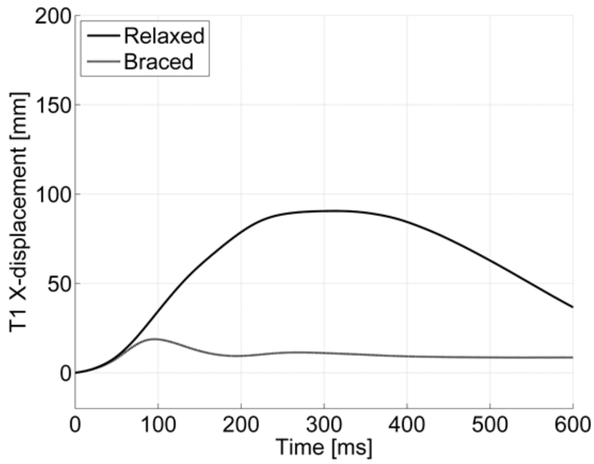

Fig. 13. T1 forward displacement of the new active human model in simulation of a relaxed and braced case.

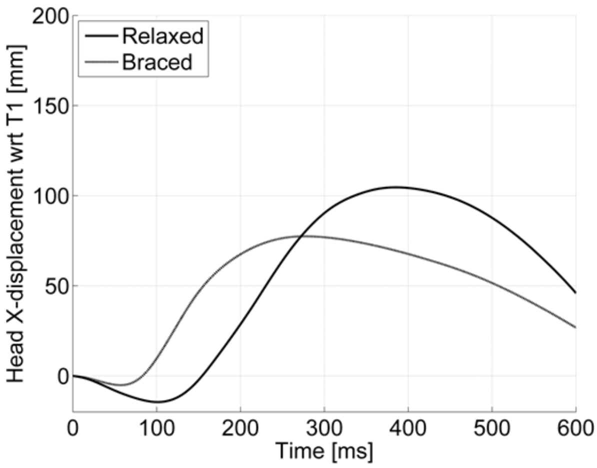

Fig. 14. Head with respect to T1 forward displacement of the new active human model in simulation of a relaxed and braced case.

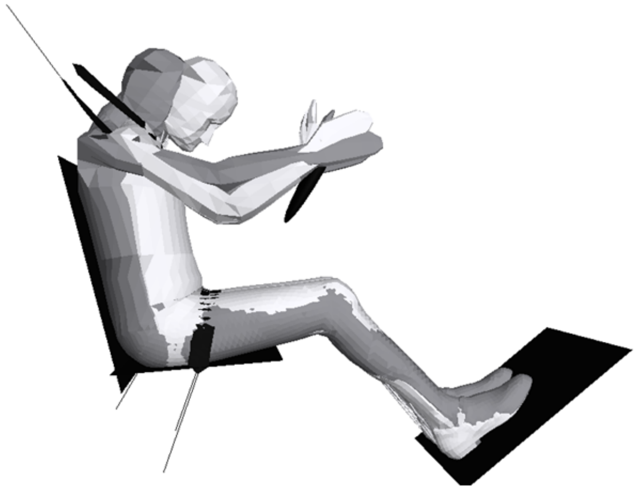

Fig. 15. Most forward position of the new active human model in the braking simulation in the relaxed (light grey) and braced (dark grey) cases.

IV. DISCUSSION

The objective of this study was to adapt the active human model to simulate realistic bracing behaviour during a car braking event. The neck of the previous active human model needed a high co-contraction level (0.5-0.9) to match response corridors of volunteers that were not instructed to brace. In addition, co-contraction was not included in the arm muscles and there was no control on the shoulder joint, while bracing of the arms was expected to have a significant effect on the head and thorax displacement of a driver in a braking event. Therefore, in this study a new neck model was developed as well as a new arm model.

The simulation results of the frequency perturbation test of the new neck model showed improved anterior-posterior head kinematics compared to the previous neck model for all frequencies. This test was simulated without co-contraction, since the co-contraction of a relaxed volunteer was expected to be very low. A limitation of the evaluation of the new neck model is that its head-neck response was compared to only one volunteer. However, this volunteer was selected from a set of 12 volunteers published in [32] to provide a representative response.

The simulation results of the arm pulse perturbation tests showed that the new arm model is capable of predicting the arm movement of a volunteer in braced as well as in relaxed condition. A limitation of the new arm model is that co-contraction was included only in the triceps and brachialis muscles. This results in reduced elbow bracing capability for flexion-extension motion and no bracing properties for pronation-supination movement. Moreover, the pronation-supination behaviour of the elbow joint is not evaluated. However, flexion-extension stabilisation and bracing is more important than pronation-supination for simulating bracing in automotive situations. Another limitation is that Hill-type muscles were not included in shoulder joint control. Thus, the controlling of the shoulder joint as modelled here has a limited biomechanical background. Also, the posterior-anterior and superior-inferior translational movement of scapula and clavicle of the new arm model has not been not evaluated. Similar as for the new neck model, a limitation of the evaluation of the new arm model is that it was compared to only one volunteer.

The braking simulation showed the importance of the effect of arm bracing for the head and thorax forward displacement. As such, bracing of the arms is an important feature for a human model in simulations of braking, and possibly as well in simulations of other pre-crash situations. Although the behaviour of the neck and arm models showed realistic responses, the whole body behaviour during a braking event should be compared to the responses of relaxed and braced volunteers, e.g. the volunteer tests of [23].

V. CONCLUSION

The new active human model with improved musculature better captured the volunteer response in an anterior-posterior frequency perturbation volunteer test than the previous model. The simulation results of the arm pulse perturbation tests showed that the new arm model is capable of predicting the arm movement of a volunteer in braced as well as in relaxed condition. A simulation of a braking event with the new active human model showed that bracing has a significant effect on the head and thorax displacement, and was mostly caused by arm bracing. Therefore, from this study it is concluded that the new neck and new arm model improved the active human model for the development of active safety systems.

VI. ACKNOWLEDGEMENT

The authors like to thank Esra van Dam from TNO for her assistance in this study.

VII. REFERENCES

[1] Bose D, Crandall J R, Untaroiu C D, Maslen E H, Influence of pre-collision occupant parameters on injury outcome in a frontal Collision, *Accident Analysis and Prevention*, 42:1398–1407, 2010.

[2] Woldrich M, Movement in the PRE-Crash Situation - A simulation research with a reversible PRE-SAFE® pulse system, abstract for the poster session (P24) Airbag 2010, *10th International Symposium and Exhibition on sophisticated Car Occupant Safety Systems*, 2010.

[3] Merz U, Schöneburg R, Fehring M, Bachmann R, Heinrich T, PRE-SAFE® IMPULSE – Early interacting occupant restraint system, *Proceedings of the 23rd International Technical Conference on the Enhanced Safety of Vehicles (ESV)*, Paper Number 13-0380, Seoul, South-Korea, 2013.

[4] Mages M, Seyffert M, Class U, Analysis of the pre-crash benefit of reversible belt pre-pretensioning in different accident scenarios, *Proceedings of the 22nd International Technical Conference on the Enhanced Safety of Vehicles (ESV)*, Paper Number 11-0442, Washington DC-US, 2011.

[5] Beeman S M, Kemper A R, Madigan M L, Duma S M, Effects of bracing on human kinematics in low-speed frontal sled tests, *Annals of Biomedical Engineering*, 39(12):2998-3011, 2011.

[6] Ejima S, Ono K, Holcombe S, Kaneoka K, Fukushima M, A study on occupant kinematics behaviour and muscle activities during pre-impact braking based on volunteer tests, *Proceedings of the International Conference on Biomechanics of Impact (IRCOBI)*, Maastricht, The Netherlands, 2007.

[7] Carlsson S, Davidsson J, Volunteer occupant kinematics during driver initiated and autonomous braking

when driving in real traffic environments, *Proceedings of the International Conference on Biomechanics of Injury (IRCOBI)*, Krakow, Poland, 2011.

[8] Meijer R, Hassel E van, Broos J, Elrofai H, van Rooij L, van Hooijdonk P, Development of a multi-body human model that predicts active and passive human behaviour, *Proceedings of the International Conference on Biomechanics of Injury (IRCOBI)*, Dublin, Ireland, 2012.

[9] Meijer R, Elrofai H, Broos J, Hassel E van, Evaluation of an active multi-body human model for braking and frontal crash events, *Proceedings of the 23rd International Technical Conference on the Enhanced Safety of Vehicles (ESV)*, Seoul, South Korea, 2013.

[10] Schöneburg R, Baumann K-H, Fehring M, The efficiency of PRE-SAFE Systems in pre-braked frontal collision situations, *Proceedings of the 22nd International Technical Conference on the Enhanced Safety of Vehicles (ESV)*, paper number 11-0302-O, Washington DC, USA, 2011.

[11] Arbogast K, Balasubramanian S, Seacrist T, Maltese M R, García-España J F, et.al., Comparison of kinematic responses of the head and spine for children and adults in low-speed frontal sled tests, *Proceedings of the 53rd Stapp Car Crash Conference*, Savannah, Georgia, USA, 2009.

[12] Thunnissen J, Wismans J, Ewing C, Thomas D, Human volunteer head-neck response in frontal flexion: A new analysis, *Society of Automotive Engineers (SAE)*, Paper 952721, *Proceedings of the 39th Stapp Car Crash Conference*, Coronado CA, USA, 439-460, 1995.

[13] Wismans J, Spenny C H, Performance Requirements for Mechanical Necks in Lateral Flexion, *Proceedings of the 27th Stapp Car Crash Journal*, San Diego, USA, 137-148, 1983.

[14] Ono K, Inami S, Kaneoka K, Gotou T, Kisanuki Y, Sakuma S, Miki K, Relationship between localized spine deformation and cervical vertebral motions for low speed rear impacts using human volunteers, *Society of Automotive Engineers (SAE)*, Paper 1999-13-0010, *Proceedings of International Conference on Biomechanics of Impact (IRCOBI)*, Sitges, Spain, 1999.

[15] Don B van, Ratingen M van, Bermond , Masson C, Vezin P, Biofidelity Impact Response Requirements for an Advanced Mid-Sized Male Crash Test Dummy, *Proceedings of the 18th International Technical Conference on Enhanced Safety of Vehicles*, Nagoya, Japan, 2003.

[16] Bouquet R, Ramet M, Bermond F, Cesari D, Thoracic and pelvis human response to impact, *Proceedings of the 14th International Technical Conference On Enhanced Safety of Vehicles (ESV)*, Munich, Germany, 100-109, 1994.

[17] Kroell C K, Schneider D C, Nahum M, Impact tolerance and response of the human thorax, *Society of Automotive Engineers (SAE)*, Paper 710851, *Proceedings of the 15th Stapp Car Crash Conference*, 163-213, 1971.

[18] Kroell C K, Schneider D C, Nahum M,. Impact tolerance and response of the human thorax II, *Society of Automotive Engineers (SAE)*, Paper 741187, *Proceedings of the 18th Stapp Car Crash Conference*, 215-253, 1974.

[19] Kroell C K, Thoracic Response to Blunt Frontal Loading, *Society of Automotive Engineers (SAE)*, Paper 67, 49-77, 1976.

[20] Nahum A, Gadd C, Schneider D, Kroell C, Deflection of the Human Thorax Under Sternal Impact, *Society of Automotive Engineers (SAE)*, Paper 700400, *Proceedings of the International Automobile Safety Conference*, 797-807, 1970.

[21] Nahum A, Schneider D, Kroell C, Cadaver skeletal response to blunt thoracic impact, Society of Automotive Engineers (SAE) Paper 751150, *Proceedings of the 19th Stapp Car Crash Conference*, 259-293, 1975.

[22] Cavanaugh J M, Nyquist G W, Goldberg S J, King A I, Lower abdominal tolerance and response, *Society of Automotive Engineers (SAE)*, Paper 861878, 41-63, 1986.

[23] Ejima S, Zama Y, Satou F, Holcombe S, Ono K, Kaneoka K, Shiina I, Prediction of the physical motion on human body based on muscle activities during pre-impact breaking, *Proceedings of the International Conference on Biomechanics of Impact (IRCOBI)*, Bern, Switzerland, 2008.

[24] Jakobsson L, Lundgren K, Norin H, Svensson M, Evaluation criteria for AIS 1 neck injuries in frontal impacts – A parametric study combining field data and madymo modeling, *Traffic Injury Prevention*, 5:374-381, 2004.

[25] MADYMO Human Body Models Manual, Version 7.4.1., TASS B.V., Rijswijk, The Netherlands, 2012.

[26] MADYMO Theory Manual, Version 7.4.1, TASS B.V., Rijswijk, The Netherlands, 2012.

[27] Winters J M, Stark L , Estimated mechanical properties of synergistic muscles involved in movements of a variety of human joints, *Journal of Biomechanics*, 21:1027-1041, 1988.

[28]Nemirovski N, van Rooij L, A new methodology for biofidelic head-neck postural control, *Proceedings of the International Conference on Biomechanics of Injury (IRCOBI)*, Hannover, Germany, 2010.

[29]Borst J, Forbes P A, Happee R, Veeger D H, Muscle parameters for musculoskeletal modelling of the human neck, *Clinical Biomechanics*, 26(4):343-394, 2011.

[30]Veldpaus F E, Woltring H J, Dortmans L J M G, A least-squares algorithm for the equiform transformation from spatial marker coordinates, *Journal of Biomechanics*, 21(1):45-54, 1988.

[31]Ackerman M J, The visible human project, *Proceedings of the Institute of Electrical and Electronics Engineers (IEEE),* 86(3):504-511, 1998.

[32]Forbes P A, de Bruijn E, Schouten A C, van der Helm F C T, Happee R, Dependency of human neck reflex responses on the bandwidth of pseudorandom anterior-posterior torso perturbations, *Experimental Brain Research*, 226(1): 1-14, 2013.

[33]Pintelon R, Schoukens J, System Identification: A Frequency Domain Approach, *Institute of Electrical and Electronics Engineers (IEEE) Press*, Piscataway, NJ, USA, 2001.

[34]Dul J, Townsend M A, Shiavi R, Johnson G E, Muscular synergism—I. On criteria for load sharing between synergistic muscles, *Journal of Biomechanics*, 17(9):663-673, 1984.

[35]van Vliet B, de Vlugt E, Happee R, Nonlinear 2D arm dynamics in response to continuous and pulse-shaped force perturbations, submitted for publication.